

钱兵, 张照伟, 张志炳, 等. 柴达木盆地西北缘牛鼻子梁镁铁-超镁铁质岩体年代学及其地质意义[J]. 中国地质, 2015, 42(3): 482–493.
Qian Bing, Zhang Zhaowei, Zhang Zhibing, et al. Zircon U-Pb geochronology of Niubiziliang mafic-ultramafic intrusion on the northwest margin of Qaidam Basin, Qinghai[J]. Geology in China, 2015, 42(3): 482–493(in Chinese with English abstract).

柴达木盆地西北缘牛鼻子梁镁铁-超镁铁质岩体 年代学及其地质意义

钱 兵¹ 张照伟¹ 张志炳² 邵 继³

(1. 国土资源部岩浆作用成矿与找矿重点实验室, 中国地质调查局西安地质调查中心, 陕西 西安 710054;
2. 中国地质大学(北京), 北京 100083; 3. 青海省核工业地质局, 青海 西宁 810008)

提要:柴达木盆地西北缘新发现的牛鼻子梁铜镍矿床位于阿尔金南缘断裂和柴北缘断裂交汇部位。矿区包含3个镁铁-超镁铁岩体, 其中Ⅱ、Ⅲ号岩体中可见铜、镍硫化物矿化, 区内岩体岩相分带明显, 由南往北可分为橄榄岩相、辉石岩相和辉长岩相。橄榄岩相岩石包含角闪二辉橄榄岩、角闪橄榄岩、二辉橄榄岩、斜长二辉橄榄岩, 辉石岩相岩石包含橄榄二辉岩、二辉岩。镍、铜矿化与橄榄岩相岩石关系密切。本文利用LA-ICP-MS锆石U-Pb同位素定年法测得Ⅰ号岩体闪长岩形成年龄为(388.0 ± 2.8) Ma, Ⅱ号矿化岩体二辉橄榄岩形成年龄为(402.2 ± 2.8) Ma, Ⅲ号矿化岩体斜长二辉橄榄岩形成年龄为(402.8 ± 2.6) Ma。属早泥盆世, 表明牛鼻子梁岩体形成于造山后陆内拉张环境, 为晚古生代早期幔源岩浆活动的产物。牛鼻子梁铜镍矿床是中国除了夏日哈木矿床外又一形成于早泥盆世新的铜镍矿化类型, 具有较好的镍铜硫化物矿床成矿潜力。

关 键 词:镁铁-超镁铁质岩; 锆石U-Pb定年; 镍铜矿化; 牛鼻子梁; 柴达木西北缘

中文分类号:P581 **文献标志码:**A **文章编号:**1000-3657(2015)03-0482-12

Zircon U-Pb geochronology of Niubiziliang mafic-ultramafic intrusion on the northwest margin of Qaidam Basin, Qinghai

QIAN Bing¹, ZHANG Zhao-wei¹, ZHANG Zhi-bing², SHAO Ji³

(1. Key Laboratory for the Study of Focused Magmatism and Giant Ore Deposits, MLR, Xi'an Institute of Geology and Mineral Resources, Xi'an 710054, Shaanxi, China; 2. China University of Geosciences, Beijing 100083, China; 3. Qinghai Geological Survey of Nuclear Industry, Xining 810008, Qinghai, China)

Abstract: The newly-discovered Niubiziliang Ni-Cu deposit is located in the intersection part of the Altum southern fault zone and the Qaidam northern fault zone, Northwest China. There are three mafic-ultramafic intrusions, of which No. Ⅱ and No. Ⅲ intrusions are Ni-Cu sulfide-bearing intrusions. The intrusions consisted of, from the south to the north, peridotite facies, pyroxenite facies and gabbro facies. The peridotite facies contains hornblende lherzolite, hornblende peridotite, lherzolite and

收稿日期:2015-01-27; 改回日期:2015-03-06

基金项目:中国地质调查局地质大调查项目(1212011121092、1212011120183 和 12120114044401)、国土资源部公益性行业科研专项项目(201511020)联合资助。

作者简介:钱兵,男,1985年生,助理研究员,研究方向为成矿作用及成矿规律;E-mail: qianbin219@163.com。

plagioclase lherzolite, the pyroxenite facies contains olivine websterite and websterite, and the peridotite facies consists of Ni-Cu bearing rocks. High-precision LA-ICP-MS zircon U-Pb dating yielded the concordant ages of 388.0 ± 2.8 Ma, 402.2 ± 2.8 Ma and 402.8 ± 2.6 Ma for diorites of No. I intrusion, lherzolites of No. II ore-bearing intrusion and plagioclase lherzolite of No. III ore-bearing intrusion, respectively. Regional tectonic evolution background indicates that the Niubiziliang rocks were formed in a post-orogenic extension environment in early Devonian and that the magma originated from mantle material. The Niubiziliang mafic-ultramafic intrusions are new type rocks containing nickel mineralization, and they have good potential for Ni-Cu sulfide exploration.

Key words: mafic-ultramafic intrusion; zircon U-Pb age; Ni-Cu mineralization; Niubiziliang; northwest margin of Qaidam Basin
About the first author: QIAN Bing, male, born in 1985, assistant researcher, engages in the study of mineralization and metallogenetic regularity; E-mail: qianbin219@163.com.

柴达木盆地西北缘近年来在铜、镍找矿方面取得了重大进展,随着青海核工业地质局在地球物理异常查证过程中牛鼻子梁矿床的发现,区内镁铁-超镁铁质小岩体越来越受到重视,至今已相继发现了大通沟南山、青新界山西、柴达木大门口、盐场北山等多处与镍矿化有关的基性-超基性岩体。牛鼻子梁岩体是区内目前发现镍矿化较好的岩体之一,前人对其岩体类型、原始岩浆、岩浆含水量、同化混染程度等成矿条件进行了初步研究^[1],认为该岩体具有形成铜镍硫化物的良好条件,成矿潜力较大。但是对于该岩体的年代学研究工作还相对甚少,前人对区内I号岩体中出露的辉长岩进行锆石U-Pb同位素测年工作,认为矿床的成岩成矿时代为晚泥盆世(367 Ma, 361 Ma)^[1, 2]。而大量的研究表明,与铜镍硫化物矿床有关的镁铁-超镁铁质岩浆在上升过程中都经历了多期次多阶段的侵位过程^[3-11],而辉长岩是同一期次岩浆在上升过程中通过分异作用在较晚阶段形成^[7, 12-15],其结晶年龄能否代表镍矿化的形成时间还需其他证据的支持。笔者通过开展牛鼻子梁矿区大比例尺地质填图及精细剖面测量工作,对区内基性-超基性岩体的岩石类型、岩相分带等进行了详细划分,初步查明前人测试所采集的辉长岩仅以脉状形式分布于I号岩体闪长岩中,均未见明显矿化,该辉长岩的结晶年龄可能并不能代表镍矿化形成时间。区内与镍矿化有关的基性-超基性岩体的形成时代还需进一步精确厘定,其形成背景等问题尚需深入研究探讨。

本文以牛鼻子梁矿床为研究对象,在野外精细大比例尺路线地质调查及室内光薄片鉴定工作基础上,选取与成矿有关的I、II、III号超基性岩体进行锆石U-Pb定年工作,厘定含矿岩体的形成时代,

探讨其形成背景。

1 区域地质背景

牛鼻子梁铜镍矿床位于柴达木盆地西北缘,阿尔金断裂南侧,大地构造位置上处于柴达木陆块西北缘早古生代后造山磨拉石前陆盆地的边缘部位(图1-a)。区内出露地层主要为古元古代金水口岩群和第四系坡积物,金水口岩群整体呈北东向展布,广泛分布于阿尔金南缘断裂南侧。按其产状和岩石类型,分上下2个岩性段,下岩性段岩性为眼球状或条带状混合岩化片麻岩、混合岩化中长片麻岩、黑云角闪斜长片麻岩、黑云斜长变粒岩和斜长角闪岩;上岩性段岩性为透辉石大理岩、石英岩、含石墨(透闪石)石英岩、黑云斜长石英片岩、绿泥石片岩。区内构造活动强烈,由于受北东向阿尔金深大断裂和北西向柴达木北缘断裂影响,区内以发育北东向、近东西向断裂为特征,多为后期破碎构造^[16]。区内岩浆活动强烈,以中酸性侵入岩类为主,其次为基性、超基性岩类,多为加里东、华力西期岩浆作用的产物。其中,镁铁-超镁铁质侵入岩呈北东向带状分布,侵位于古元古代金水口岩群中,从西向东依次分布有牛鼻子梁、大通沟南山、青新界山西、柴达木大门口、盐场北山和盐场北山东等多个岩体(图1-b)。

2 岩体特征

2.1 岩体及含矿性特征

牛鼻子梁岩体位于研究区西南部(图1-b),区内出露地层为古元古代金水口岩群和第四系(图2)。区内断裂构造发育,以北东向、近东西向和北东向3组断裂为主,其中北东向断裂对区内基性-超

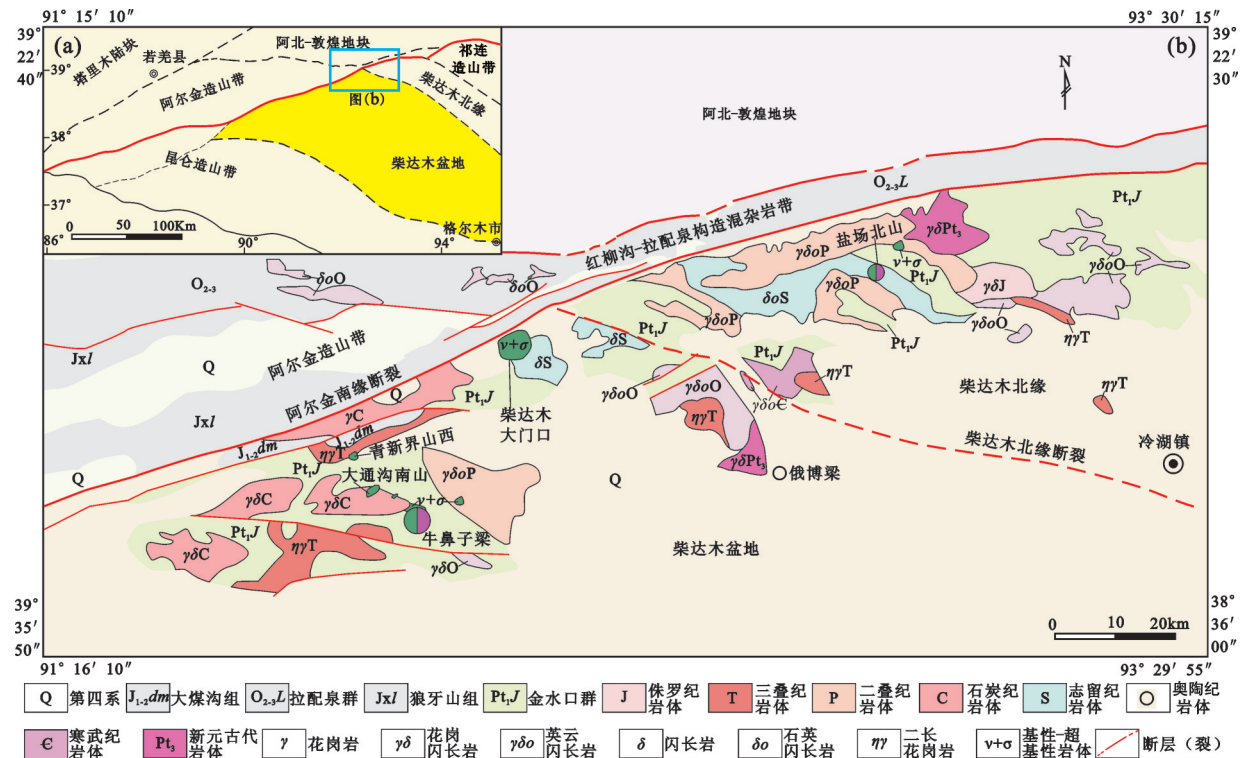


图1 柴达木盆地区域大地构造简图(a)及柴达木西北缘区域地质图(b)

Fig.1 Regional tectonic sketch map of Qaidam Basin (a) and regional geological map of the northwest margin of Qaidam Basin (b)

基性岩体的侵入具有十分重要的控制作用,而近东-西向和北西向断裂多为后期破碎构造,致使岩体在深部出现不连续的现象^①。区内出露的侵入岩为花岗闪长岩、闪长岩、钾长花岗岩和镁铁-超镁铁质岩体(图2),中酸性岩类主要分布于矿区北部和南部,南部出露的岩体主要为形成于古元古代糜棱岩化花岗闪长岩,北部则为泥盆纪闪长岩和三叠纪钾长花岗岩。镁铁-超镁铁质岩体分布于矿区中部,按其产出形态可分为Ⅰ、Ⅱ、Ⅲ三个岩体(图2),其中与镍矿化有关的岩体为Ⅱ、Ⅲ号岩体。

I号岩体位于矿区中部,平面形态呈长条状(图2),长轴北西向,长约6 km,最大宽度约1.5 km。岩性主要为闪长岩,局部零星夹杂辉长岩脉。岩石发生了一定程度的蚀变作用,主要有绿泥石化、透闪石化及褐铁矿化。局部地段闪长岩中可见星点状黄铁矿化,为后期热液成因。岩体中均未见明显镍、铜矿化。

II号岩体位于牛鼻子梁铜镍矿区的西部,北西

向延伸,长680 m,宽20~250 m。岩性为角闪二辉橄榄岩、角闪橄榄岩、橄榄二辉岩(图2),角闪橄榄岩发生了强烈的蛇纹石化。目前该岩体中发现铜镍矿体4条,矿体赋存于橄榄二辉岩和角闪橄榄岩中,长40~160 m,厚1.62~22 m。Cu平均品位0.22%~0.79%,Ni平均品位0.20%~1.57%,伴生Co最高品位0.08%,平均品位0.03%。规模最大的一条矿体视厚度达41.1 m,镍平均品位0.56%,最高1.57%。矿石以稀疏浸染状、星点状构造为主,矿石矿物主要为磁黄铁矿、镍黄铁矿和少量黄铜矿。

III号岩体呈北西向延伸,南东侧伏,长1000 m,宽20~250 m,岩性为橄榄二辉岩、二辉岩、二辉橄榄岩、斜长二辉橄榄岩、辉长岩和闪长岩等(图2),辉石岩相和橄榄岩相岩石发生了不同程度的蛇纹石化。III号岩体已发现铜镍矿(化)体6条,矿体赋存于橄榄二辉岩、二辉岩和二辉橄榄岩中,视厚度为1.1~5.16 m,Ni品位0.3%~0.478%,共生有铜钴。矿石呈块状、浸染状、稀疏浸染状为主,矿石矿物为镍

^①王永刚,申大利,张师祥,等.青海省茫崖行委牛鼻子梁铜镍矿2009—2010普查报告[R].青海核工业地质局,2012.

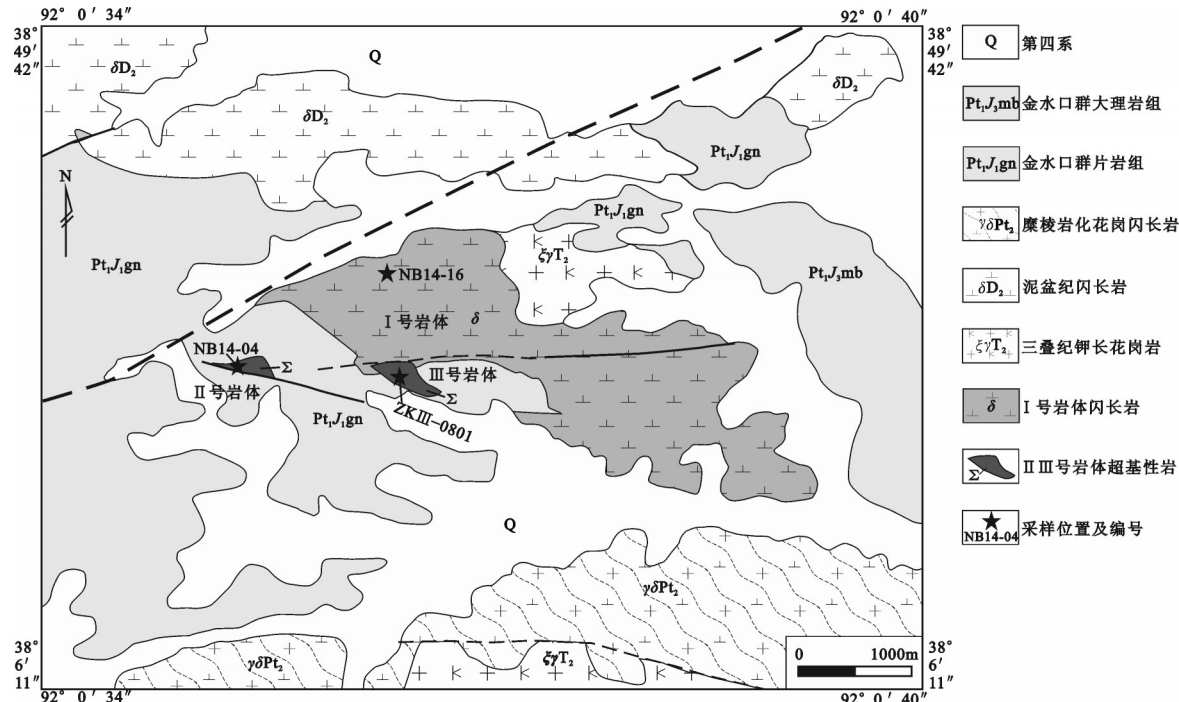


图2 柴达木西北缘牛鼻子梁矿区地质图

Fig.2 Geological sketch map of the Niubiziliang deposit on the northwest margin of Qaidam Block

黄铁矿、磁黄铁矿和少量黄铜矿。Ⅲ号岩体和Ⅰ号岩体呈侵入接触关系,野外可见Ⅰ号岩体闪长岩呈脉状侵位于Ⅲ号岩体二辉岩、橄榄二辉岩中,明显晚于Ⅲ号岩体的形成时间。

2.2 岩相分带及岩石类型

通过野外地质路线调查工作,结合区内岩石的接触关系及光薄片鉴定结果,本次对区内出露的岩体岩相进行了详细的划分(图3)。Ⅱ号岩体由橄榄岩相和辉石岩相岩石组成,深部向北侧伏(图3-a)。橄榄岩相分布于岩体南侧,以角闪橄榄岩、角闪二辉橄榄岩为主,辉石岩相分布于岩体北部,以橄榄二辉岩为主。在北侧橄榄岩相岩石与金水口岩群斜长片麻岩接触部位,可见磁黄铁矿化、黄铜矿化。Ⅲ号岩体由南往北基性程度逐渐降低,分别为橄榄岩相、辉石岩相和辉长岩类。岩体整体呈漏斗状,深部逐渐缩小(图3-b)。橄榄岩相由二辉橄榄岩和斜长二辉橄榄岩组成,辉石岩相为橄榄二辉岩和二辉岩组成,辉长岩相由角闪辉长岩、辉长岩组成。在橄榄岩相岩石靠近地层部位可见磁黄铁矿体。

角闪二辉橄榄岩呈堆晶结构、块状构造。岩石由橄榄石(45%~65%)、斜方辉石(8%~20%)、单斜辉

石(5%~15%)和角闪石(3%~8%)组成。橄榄石呈堆晶结构,自形-半自形粒状,粒径0.15~0.25 mm,裂理发育,沿裂理方向蛇纹石化较强,部分可见大量铁质析出。斜方辉石呈半自形粒状,粒径0.20~0.50 mm,包橄结构明显,蛇纹石化强烈。单斜辉石呈填隙相分布于橄榄石或斜方辉石粒间,呈半自形-他形粒状,粒径0.15~0.40 mm,部分透闪石化、绿泥石化强烈。角闪石呈半自形-他形柱状,粒径0.15~0.30 mm,表面发生强烈绿泥石化。

斜长二辉橄榄岩呈包橄结构、块状构造。岩石由橄榄石(40%~60%)、斜方辉石(5%~20%)、单斜辉石(5%~20%)和斜长石(5%~8%)组成。橄榄石呈浑圆状,粒径0.20~0.30 mm,边部蛇纹石化强烈。斜方辉石和单斜辉石基本相同,呈半自形粒状,包橄结构明显,单斜辉石表面发生了强烈的透闪石化、绿泥石化。斜长石呈半自形粒状,粒径0.10~1.00 mm,大部分充填于橄榄石颗粒间,少数被斜方辉石和单斜辉石包裹,与橄榄石基本同时结晶形成。

橄榄二辉岩呈包橄结构、块状构造。岩石由橄榄石(20%~40%)、斜方辉石(15%~30%)、单斜辉石(15%~30%)组成。橄榄石呈自形-半自形浑圆状,

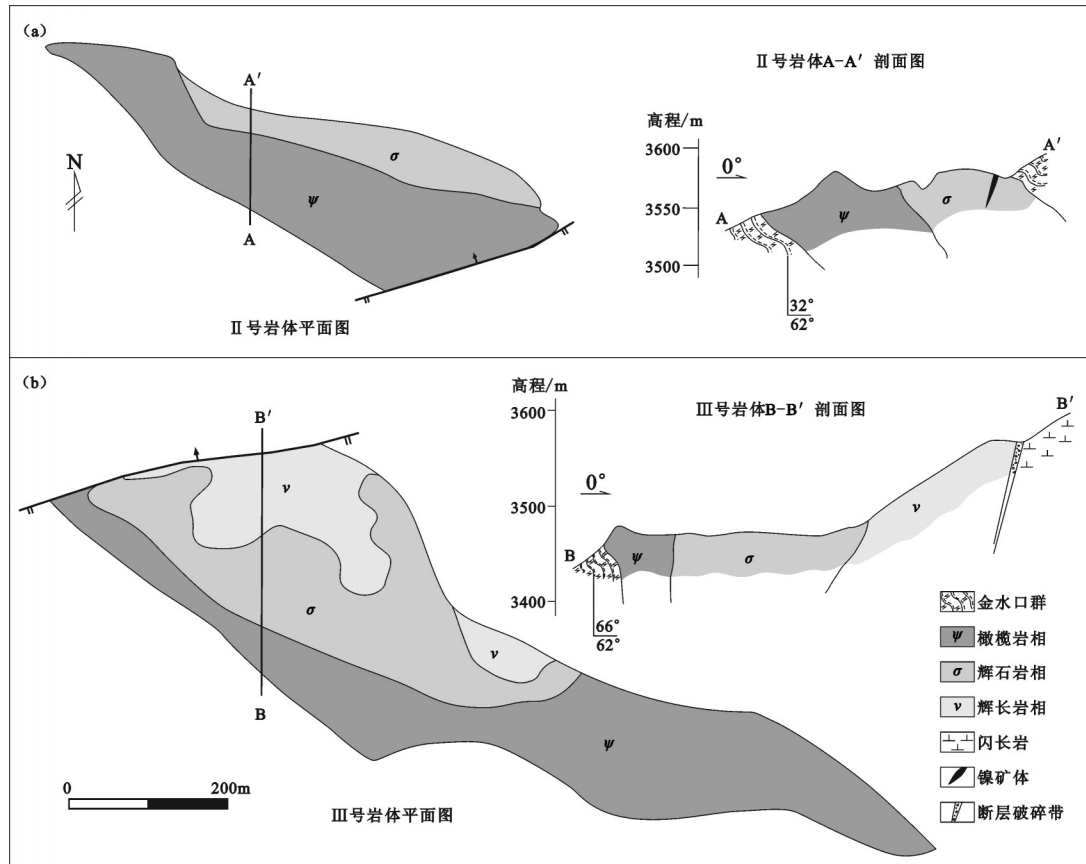


图3 牛鼻子梁矿区Ⅱ、Ⅲ号镁铁-超镁铁质岩体岩相分带示意图
Fig.3 The facies of No. Ⅱ, Ⅲ mafic-ultramafic intrusions in Niubiziliang deposit

粒径0.10~0.30 mm,部分颗粒完全蛇纹石化,表面析出大量铁质。斜方辉石和单斜辉石含量基本相同,半自形粒状,0.10~0.40 mm,包橄榄结构明显,斜方辉石表面蛇纹石化强烈,单斜辉石局部发生强烈绿泥石化、透闪石化。

辉长岩呈辉长结构,块状构造。岩石由单斜辉石(45%~60%)、斜长石(50%~55%)及少量普通角闪石(0~5%)和少量石英组成。单斜辉石以普通辉石为主,呈自形短柱状结构,粒径0.20~0.30 mm,部分颗粒边部发生透闪石化、绿泥石化。斜长石含量与辉石基本相同,粒径0.20~0.40 mm,聚片双晶发育,与辉石组成辉长结构。普通角闪石少量分布,局部颗粒表明发生强烈绿泥石化。

3 样品测试及分析结果

3.1 样品测试

本次分别选取了牛鼻子梁矿床Ⅰ号岩体中的

闪长岩(NB14-16)、Ⅱ号岩体中的二辉橄榄岩(NB14-04)、Ⅲ号岩体中的斜长二辉橄榄岩(ZKⅢ-0801)进行锆石U-Pb同位素测年工作。锆石单矿物分选工作在河北省区域地质矿产调查研究所实验室完成。锆石CL图像在西北大学大陆动力学国家重点实验室电子探针仪加载的阴极发光仪上完成。锆石LA-ICP-MS U-Pb定年测试分析在中国地质科学院矿产资源研究所国土资源部成矿作用与资源评价重点实验室完成,定年分析仪器为Finnigan Neptune型ICP-MS及与之配套的Newwave UP 213激光剥蚀系统。激光剥蚀束斑直径为40 μm,以He为载气。对锆石标准的定年精度和准确度在1%(2s)左右,锆石U-Pb定年以锆石GJ-1为外标,U、Th含量以锆石M127(U: 923×10⁻⁶; Th: 439×10⁻⁶; Th/U: 0.475)^[17]为外标进行校正。数据处理采用ICPMSCal程序^[18],锆石年龄及谐和图绘制用Isoplot 3.0程序。详细分析步骤和数据处理方

法见侯可军等^[19]。

3.2 分析结果

I号岩体闪长岩(NB14-16)中锆石呈自形-半自形柱状,粒径较大,为150~400 μm,长宽比为1.5:1~3:1。阴极发光照片显示锆石内部发育较为清晰的岩浆震荡环带(图4-a),Th/U比值变化范围介于0.66~1.54(表1),均远高于0.1,为岩浆成因锆石^[20]。样品在进行普通铅校正后的有效数据点为24个,²⁰⁶Pb/²³⁸U表面年龄为(380.9±3.5) Ma~(395.7±4.2) Ma,加权平均年龄为(388.0±1.8) Ma(MSWD=0.89),分析数据在²⁰⁶Pb/²³⁸U-²⁰⁷Pb/²³⁵U谐和图上均落在谐和线上或其附近(图4-a),表明牛鼻子梁I号岩体闪长岩结晶年龄为(388.0±1.8) Ma,属于中泥盆世。

II号岩体二辉橄榄岩(NB14-04)中锆石为柱状,粒径为70~200μm,长宽比为1:1~2:1。锆石多为浑圆状,内部可见较清晰的岩浆震荡环带(图4-b),Th/U比值变化范围介于0.45~2.71(表1),均远高于0.1,为岩浆成因锆石。样品在进行普通铅校正后的有效数据点为19个,²⁰⁶Pb/²³⁸U表面年龄为(396.2±14.1) Ma~(406.2±6.9) Ma,加权平均年龄为(402.2±2.8) Ma(MSWD=0.22),在²⁰⁶Pb/²³⁸U-²⁰⁷Pb/²³⁵U谐和图上分析数据均落在谐和线上(图4-b),表明牛鼻子梁I号岩体闪长岩结晶年龄为(402.2±2.8) Ma,属于早泥盆世。

III号岩体斜长二辉橄榄岩(ZK III-0801)中锆石为柱状,粒径为50~150μm,长宽比为0.5:1~1.5:1。锆石以浑圆状为主,内部可见较为清晰的岩浆震荡环带(图4-c),Th/U比值变化范围介于0.46~4.88(表1),均远高于0.1,为岩浆成因锆石。样品在进行普通铅校正后的有效数据点为19个,²⁰⁶Pb/²³⁸U表面年龄为(400.3±6.5) Ma~(405.6±7.0) Ma,加权平均年龄为(402.8±2.6) Ma(MSWD=0.078),在²⁰⁶Pb/²³⁸U-²⁰⁷Pb/²³⁵U谐和图上分析数据均落在谐和线上(图4-c),表明牛鼻子梁I号岩体闪长岩结晶年龄为(402.8±2.6) Ma,与样品NB14-04得出的锆石结晶年龄在误差范围内一致,均属于早泥盆世岩浆活动的产物。

4 讨论

4.1 年代学意义

中国与铜镍矿化有关的基性-超基性岩体形成时代多集中于新元古代和晚古生代^[10, 21~25]。新元古

代岩体主要形成于大陆边缘裂谷环境,以金川岩体为代表(825 Ma)^[26, 27];晚古生代岩体产于东天山一带造山带中(298~269 Ma)^[28~33]和攀西一带大陆溢流玄武岩中(260~250 Ma)^[34~37],以新疆的喀拉通克、黄山东、图拉尔根、坡北,以及四川力马河、云南白寨为代表。近两年来,随着柴达木南缘东昆仑造山带中夏日哈木超大型镍矿床(411 Ma)的发现^[38],越来越多的地质工作者开始重视对柴达木周缘晚古生代早期含镍基性-超基性岩体的研究工作^[39]。

本次研究的牛鼻子梁岩体是柴达木西北缘近年来新发现的与镍、铜矿化有关的基性-超基性岩群的代表,年代学研究表明区内I号岩体闪长岩形成年龄为(388.0±1.8) Ma,辉长岩形成年龄为367~361 Ma^[1, 2],II号岩体二辉橄榄岩形成年龄为(402.2±2.8) Ma、III号岩体斜长二辉橄榄岩形成年龄为(402.8±2.6) Ma,均形成于泥盆纪,为晚古生代岩浆活动的产物。众所周知,在岩浆铜镍硫化物矿床形成过程中,大多数含镍、铜等硫化物在发生熔离过程中是与基性程度较高的橄榄岩相或辉石岩相等岩石同时形成。本次研究的牛鼻子梁矿床中的镍黄铁矿、磁黄铁矿等硫化物亦都赋存于二辉橄榄岩、角闪橄榄岩或橄榄二辉岩中,表明成矿与橄榄岩相岩石结晶时间基本相同,II、III号岩体的形成年龄(402 Ma)能够代表矿床形成的准确时间。而对于区内388~361 Ma时期形成的辉长岩、闪长岩等中-基性岩石,可能为含矿岩浆演化到后期由硫化物不饱和残余岩浆发生分异作用而形成的产物。牛鼻子梁晚古生代早期岩体的确定,是除了夏日哈木矿床外又一新的含镍矿化类型,为中国晚古生代早期镍矿找矿方向提供了新的证据。

4.2 成矿地质背景

牛鼻子梁岩体地处柴达木盆地北缘、阿尔金山南缘交汇的部位,复杂的地质条件致使其形成背景与相邻造山带的构造演化有着紧密不可分的关系。柴北缘造山带由于陆续在榴辉岩及其围岩片麻岩中发现了超高压变质矿物(如柯石英、金刚石等)以来^[40, 41],已成为了地学界研究的热点地区之一。众多学者基于锆石各种定年方法确定该带内高压-超高压变质岩形成时代变化范围为495~420 Ma^[42~46],确定柴北缘是一条早古生代高压-超高压变质带,主体形成于陆壳俯冲作用过程。而南阿

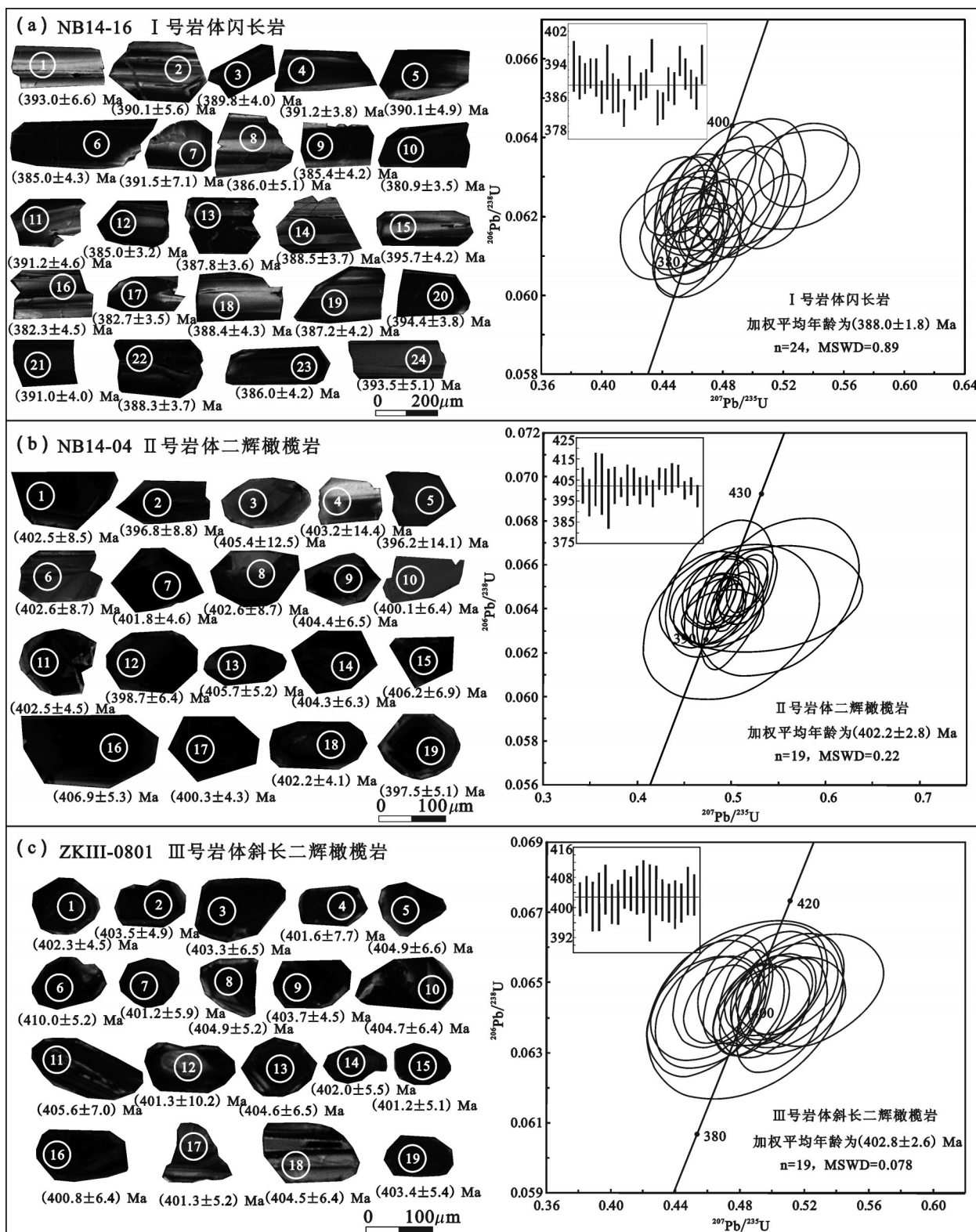


图4 牛鼻子梁矿床锆石阴极发光图及锆石U-Pb谐和图

Fig.4 Zircon CL images for micro-beam analyzed spots with apparent U-Pb ages and zircon U-Pb concordia diagram of the Niubiziliang deposit

表1 牛鼻子梁矿床镁铁-超镁铁质岩石锆石LA-ICP-MSU-Th-Pb分析结果

Table 1 Zircon LA-ICP-MS analytical data of the mafic-ultramafic intrusions in the Niubiziliang deposit

测试点	$^{232}\text{Th}/10^{-6}$	$^{238}\text{U}/10^{-6}$	Th/U	同位素比值						表面年龄 Ma					
				$^{207}\text{Pb}^{206}\text{Pb}$	1 δ	$^{207}\text{Pb}^{235}\text{U}$	1 δ	$^{206}\text{Pb}^{238}\text{U}$	1 δ	$^{207}\text{Pb}^{208}\text{Pb}$	1 δ	$^{207}\text{Pb}^{235}\text{U}$	1 δ		
NB14-16-1	129.3	195.2	0.66	0.0582	0.0028	0.4992	0.0229	0.0629	0.0011	538.9	105.5	411.2	15.5	393.0	6.6
NB14-16-2	374.1	328.2	1.14	0.0570	0.0022	0.4932	0.0200	0.0624	0.0009	500.0	52.8	407.1	13.6	390.1	5.6
NB14-16-3	1214.5	1085.9	1.12	0.0531	0.0012	0.4593	0.0109	0.0623	0.0007	331.5	51.8	383.8	7.6	389.8	4.0
NB14-16-4	753.5	575.8	1.31	0.0528	0.0014	0.4571	0.0124	0.0626	0.0006	320.4	65.7	382.2	8.6	391.2	3.8
NB14-16-5	806.4	663.2	1.22	0.0533	0.0019	0.4595	0.0162	0.0624	0.0008	342.7	86.1	383.9	11.3	390.1	4.9
NB14-16-6	1483.1	1000.8	1.48	0.0533	0.0017	0.4564	0.0156	0.0615	0.0007	342.7	39.8	381.7	10.9	385.0	4.3
NB14-16-7	127.6	188.3	0.68	0.0567	0.0031	0.4829	0.0243	0.0626	0.0012	479.7	113.9	400.1	16.7	391.5	7.1
NB14-16-8	312.3	303.0	1.03	0.0525	0.0028	0.4476	0.0242	0.0617	0.0008	309.3	119.4	375.6	17.0	386.0	5.1
NB14-16-9	1234.1	800.8	1.54	0.0546	0.0018	0.4630	0.0140	0.0616	0.0007	394.5	72.2	386.4	9.7	385.4	4.2
NB14-16-10	789.5	650.9	1.21	0.0540	0.0015	0.4543	0.0129	0.0609	0.0006	368.6	64.8	380.3	9.0	380.9	3.5
NB14-16-11	291.3	339.4	0.86	0.0563	0.0025	0.4830	0.0203	0.0626	0.0008	464.9	98.1	400.1	13.9	391.2	4.6
NB14-16-12	832.8	690.7	1.21	0.0555	0.0017	0.4713	0.0136	0.0615	0.0005	431.5	66.7	392.1	9.4	385.0	3.2
NB14-16-13	948.1	628.1	1.51	0.0550	0.0016	0.4723	0.0137	0.0620	0.0006	413.0	66.7	392.8	9.5	387.8	3.6
NB14-16-14	682.5	575.3	1.19	0.0598	0.0016	0.5138	0.0142	0.0621	0.0006	594.5	26.8	421.0	9.6	388.5	3.7
NB14-16-15	369.9	406.7	0.91	0.0608	0.0022	0.5330	0.0194	0.0633	0.0007	631.5	77.8	433.8	12.8	395.7	4.2
NB14-16-16	461.1	454.7	1.01	0.0546	0.0022	0.4615	0.0186	0.0611	0.0007	398.2	90.7	385.3	12.9	382.3	4.5
NB14-16-17	1253.6	908.0	1.38	0.0547	0.0015	0.4623	0.0123	0.0612	0.0006	398.2	58.3	385.9	8.5	382.7	3.5
NB14-16-18	364.8	381.7	0.96	0.0538	0.0021	0.4620	0.0181	0.0621	0.0007	361.2	58.3	385.7	12.6	388.4	4.3
NB14-16-19	517.3	479.8	1.08	0.0559	0.0018	0.4779	0.0153	0.0619	0.0007	455.6	72.2	396.7	10.5	387.2	4.2
NB14-16-20	1164.7	1012.7	1.15	0.0556	0.0014	0.4844	0.0113	0.0631	0.0006	438.9	55.6	401.1	7.7	394.4	3.8
NB14-16-21	597.8	598.9	1.00	0.0517	0.0016	0.4476	0.0136	0.0625	0.0007	272.3	63.9	375.6	9.5	391.0	4.0
NB14-16-22	780.0	764.2	1.02	0.0537	0.0016	0.4606	0.0128	0.0621	0.0006	361.2	66.7	384.7	8.9	388.3	3.7
NB14-16-23	248.0	355.0	0.70	0.0530	0.0021	0.4513	0.0174	0.0617	0.0007	331.5	90.7	378.2	12.2	386.0	4.2
NB14-16-24	317.6	341.6	0.93	0.0610	0.0032	0.5293	0.0270	0.0629	0.0008	638.9	111.1	431.3	17.9	393.5	5.1
NB14-04-1	1714.0	1080.4	1.59	0.0546	0.0021	0.4832	0.0159	0.0644	0.0014	394.5	87.0	400.2	10.9	402.5	8.5
NB14-04-2	1491.2	1167.4	1.28	0.0568	0.0022	0.4994	0.0208	0.0635	0.0015	483.4	85.2	411.3	14.1	396.8	8.8
NB14-04-3	438.1	392.7	1.12	0.0541	0.0038	0.4874	0.0378	0.0649	0.0021	376.0	161.1	403.1	25.8	405.4	12.5
NB14-04-4	151.4	122.2	1.24	0.0636	0.0073	0.5495	0.0569	0.0645	0.0024	731.5	238.7	444.7	37.3	403.2	14.4
NB14-04-5	118.4	181.1	0.65	0.0598	0.0089	0.4995	0.0617	0.0634	0.0023	594.5	325.9	411.4	41.8	396.2	14.1
NB14-04-6	204.4	227.0	0.90	0.0535	0.0039	0.4743	0.0337	0.0644	0.0014	350.1	164.8	394.2	23.2	402.6	8.7
NB14-04-7	3098.3	1476.0	2.10	0.0555	0.0013	0.4947	0.0114	0.0643	0.0008	435.2	50.0	408.1	7.8	401.8	4.6
NB14-04-8	54.2	120.1	0.45	0.0610	0.0084	0.5367	0.0676	0.0645	0.0016	638.9	300.7	436.2	44.7	402.6	9.7
NB14-04-9	1386.6	662.5	2.09	0.0545	0.0029	0.4886	0.0273	0.0647	0.0011	394.5	88.0	403.9	18.6	404.4	6.5
NB14-04-10	405.6	287.3	1.41	0.0546	0.0033	0.4824	0.0292	0.0640	0.0011	398.2	137.0	399.7	20.0	400.1	6.4
NB14-04-11	1935.5	1172.9	1.65	0.0541	0.0014	0.4813	0.0127	0.0644	0.0007	376.0	54.6	399.0	8.7	402.5	4.5
NB14-04-12	2996.4	1589.5	1.89	0.0545	0.0022	0.4821	0.0218	0.0638	0.0010	394.5	92.6	399.5	14.9	398.7	6.4
NB14-04-13	2994.5	1106.1	2.71	0.0568	0.0019	0.5107	0.0178	0.0650	0.0009	487.1	78.7	418.9	11.9	405.7	5.2
NB14-04-14	3177.0	1691.5	1.88	0.0543	0.0024	0.4860	0.0224	0.0647	0.0010	383.4	98.1	402.2	15.3	404.3	6.3
NB14-04-15	1367.3	776.0	1.76	0.0578	0.0024	0.5172	0.0208	0.0650	0.0011	524.1	88.9	423.3	13.9	406.2	6.9
NB14-04-16	3102.3	2252.0	1.38	0.0572	0.0015	0.5165	0.0146	0.0652	0.0009	501.9	63.9	422.8	9.8	406.9	5.3
NB14-04-17	3527.1	2313.3	1.52	0.0560	0.0011	0.4968	0.0108	0.0641	0.0007	450.0	44.4	409.5	7.3	400.3	4.3
NB14-04-18	3123.5	1658.9	1.88	0.0549	0.0012	0.4882	0.0107	0.0644	0.0007	409.3	45.4	403.7	7.3	402.2	4.1
NB14-04-19	1531.2	841.0	1.82	0.0553	0.0029	0.4907	0.0287	0.0636	0.0008	433.4	118.5	405.4	19.6	397.5	5.1
ZKII-0801-1	999.5	1044.4	0.96	0.0526	0.0016	0.4668	0.0143	0.0644	0.0007	309.3	75.0	389.0	9.9	402.3	4.5
ZKII-0801-2	7271.4	4.88	0.0563	0.0020	0.5008	0.0176	0.0646	0.0008	461.2	76.8	412.2	11.9	403.5	4.9	
ZKII-0801-3	737.6	1439.3	0.51	0.0576	0.0022	0.5060	0.0186	0.0641	0.0011	522.3	85.2	415.7	12.5	400.3	6.5
ZKII-0801-4	285.8	616.4	0.46	0.0525	0.0029	0.4593	0.0239	0.0643	0.0013	305.6	125.9	383.8	16.7	401.6	7.7
ZKII-0801-5	1186.5	860.4	1.38	0.0562	0.0024	0.4991	0.0212	0.0648	0.0011	457.5	93.5	411.1	14.4	404.9	6.6
ZKII-0801-6	6834.2	2169.1	3.15	0.0555	0.0020	0.4952	0.0183	0.0642	0.0009	431.5	79.6	408.4	12.4	401.0	5.2
ZKII-0801-7	785.9	868.4	0.90	0.0517	0.0026	0.4588	0.0225	0.0643	0.0010	333.4	119.4	383.4	15.7	401.5	5.9
ZKII-0801-8	2774.1	839.8	3.30	0.0566	0.0023	0.5093	0.0210	0.0648	0.0009	476.0	88.0	418.0	14.2	404.9	5.2
ZKII-0801-9	5232.6	1438.2	3.64	0.0554	0.0020	0.4976	0.0180	0.0646	0.0007	427.8	81.5	410.1	12.2	403.7	4.5
ZKII-0801-10	1305.4	789.7	1.65	0.0586	0.0030	0.5265	0.0272	0.0648	0.0011	553.7	113.7	429.5	18.1	404.7	6.4
ZKII-0801-11	4529.6	1020.5	4.44	0.0550	0.0031	0.4940	0.0266	0.0649	0.0012	409.3	125.9	407.6	18.1	405.6	7.0
ZKII-0801-12	271.4	573.7	0.47	0.0539	0.0045	0.4835	0.0402	0.0642	0.0017	368.6	187.0	400.5	27.5	401.3	10.2
ZKII-0801-13	1119.6	1614.3	0.69	0.0569	0.0025	0.5117	0.0217	0.0648	0.0011	487.1	98.9	419.6	14.6	404.6	6.5
ZKII-0801-14	1267.9	933.8	1.36	0.0571	0.0027	0.5102	0.0233	0.0644	0.0009	494.5	105.5	418.6	15.7	402.0	5.5
ZKII-0801-15	2926.0	2428.0	1.21	0.0545	0.0017	0.4857	0.0145	0.0642	0.0008	390.8	70.4	402.0	9.9	401.2	5.1
ZKII-0801-16	488.2	556.3	0.88	0.0524	0.0028	0.4616	0.0226	0.0642	0.0011	301.9	124.1	385.			

尔金山地区近年来亦陆续发现了不同类型的超高压变质岩石^[47~49],带内产出的榴辉岩在地质背景、矿物组合、岩石地球化学、温度压力条件、退变质作用以及峰期变质时代(503~500 Ma 和 495 Ma)等方面与柴北缘造山带非常相似,该超高压变质带被认为是柴北缘的西延部分,后被阿尔金断裂左行位移了约 400 km^[50, 51]。前人研究发现南阿尔金—柴北缘构造带是由冈瓦纳大陆和西伯利亚地块间的“原特提斯洋”经洋壳俯冲、陆陆碰撞和陆壳折返的产物^[53, 54]。而在如此大规模的洋—陆转换地质作用过程中,必然会出现一系列与不同深部构造作用过程相应的独特地质体,如蛇绿岩、镁铁—超镁铁质侵入岩、花岗岩等。

前人依据柴北缘造山带中分布的大量古生代花岗岩研究工作,对造山带构造演化与花岗岩浆期次之间的关系进行了详细厘定,初步建立了洋—陆转换过程中区域构造演化格架。认为区内洋壳俯冲作用发生于 496~446 Ma^[54~56];大洋闭合—陆陆碰撞作用发生于 440~420 Ma^[57, 58];碰撞后板块折返阶段发生于 410~395 Ma^[56];造山后陆内伸展阶段发生于 383~372 Ma^[56]。本次研究的牛鼻子梁镁铁—超镁铁质岩体侵位于柴达木西北缘古元古代金水口岩群中,形成于 402~361 Ma,对应于区内构造演化过程中的碰撞造山晚期至造山后的张性环境。同时区内泥盆纪地层也为一套山前或山间盆地的粗碎屑岩,属磨拉石相沉积,是造山后不同块体之间滑塌、伸展后形成的,也显示牛鼻子梁矿床形成于造山后拉张裂解的环境。

5 结 论

(1) 牛鼻子梁岩体岩相分带明显,由南往北可分为橄榄岩相、辉石岩相、辉长岩类。橄榄岩相岩石包含角闪二辉橄榄岩、角闪橄榄岩、二辉橄榄岩、斜长二辉橄榄岩,辉石岩相岩石包含橄榄二辉岩、二辉岩组。镍、铜矿化均赋存与橄榄岩相岩石中。

(2) 锆石 U-Pb 同位素测年法测得 I 号岩体闪长岩形成年龄为(388.0±2.8) Ma, II 号矿化岩体二辉橄榄岩形成年龄为(402.2±2.8) Ma, III 号矿化岩体斜长二辉橄榄岩形成年龄为(402.8±2.6) Ma, 均为晚古生代早期岩浆活动的产物。成矿时代与橄榄岩相岩石形成时间一致,为 402 Ma。

(3) 牛鼻子梁岩体形成于早古生代柴北缘洋—陆转换造山作用过程中的后造山张性环境,具有良好的镍矿成矿潜力。

致谢:野外工作得到了青海省核工业地质局第二地质大队的野外一线工作人员王永刚工程师、才让助理工程师等人的大力协助,样品测试和数据处理过程中得到了中国地质科学院侯可军助理研究员、孙涛助理研究员的帮助,文稿撰写中审稿专家和编辑部李亚萍老师提出了宝贵的修改意见,在此一并表示衷心的感谢。

参 考 文 献(References):

- [1] 凌锦兰, 赵彦锋, 康珍, 等. 柴达木地块北缘牛鼻子梁镁铁质—超镁铁质岩体岩石成因与成矿条件[J]. 岩石学报, 2014, 30(6): 1628~1646.
Lin Jinlan, Zhao Yanfeng, Kang Zhen, et al. Petrogenesis and mineralization of Niubiziliang mafic—ultramafic intrusion in the northern margin of Qaidam Block, NW China[J]. Acta Petrologica Sinica, 2014, 30(6): 1628~1646 (in Chinese with English abstract).
- [2] 刘会文, 王雪萍, 邵继, 等. 牛鼻子梁镁铁质—超镁铁质杂岩体岩石特征[J]. 矿床地质, 2014, 33(1): 87~103.
Liu Huiwen, Wang Xueping, Shao Ji, et al. Rock characteristics of Niubiziliang mafic—ultramafic complex[J]. Mineral Deposits, 2014, 33(1): 87~103 (in Chinese with English abstract).
- [3] 汤中立, 闫海卿, 焦建刚, 等. 中国岩浆硫化物矿床新分类与小岩体成矿作用[J]. 矿床地质, 2006, 25(1): 1~9.
Tang Zhongli, Yan Haiqing, Jiao Jiangang, et al. New classification of magmatic sulfide deposits in China and ore-forming processes of small intrusive bodies[J]. Mineral Deposits, 2006, 25(1): 1~9 (in Chinese with English abstract).
- [4] Ripley E M. Sulfur isotopic studies of the Dinka Road Cu—Ni deposit, Duluth Complex, Minnesota[J]. Economic Geology, 1981, 76(3): 610~620.
- [5] Chai G, Naldrett A J. Characteristics of Ni—Cu—PGE mineralization and genesis of the Jinchuan deposit, northwest China[J]. Economic Geology, 1992, 87(6): 1475~1495.
- [6] Li C S, Xu Z H, J W S, et al. Compositional variations of olivine from the Jinchuan Ni—Cu sulfide deposit, western China: implications for ore genesis[J]. Mineralium Deposita, 2004, 39(2): 159~172.
- [7] Naldrett A. World-class Ni—Cu—PGE deposits: key factors in their genesis[J]. Mineralium Deposita, 1999, 34(3): 227~240.
- [8] Naldrett A J. Magmatic Sulfide Deposits: Geology, Geochemistry and Exploration[M]. Springer, 2004: 1~728.
- [9] 汤中立. 中国岩浆硫化物矿床的主要成矿机制[J]. 地质学报, 1996, 70(3): 237~243.
Tang Zhongli. The main mineralization mechanism of magma

- sulfide deposits in China[J]. *Acta Geologica Sinica*, 70(3): 237–243 (in Chinese with English abstract).
- [10] 李文渊. 岩浆 Cu–Ni–PGE 硫化物矿床研究现状及发展趋势[J]. 西北地质, 2007, 40(2): 1–28.
Li Wenyuan. The current status and prospect on magmatic Ni–Cu–PGE deposits[J]. *Northwestern Geology*, 2007, 40(2): 1–28 (in Chinese with English abstract).
- [11] 李文渊. 中国铜镍硫化物矿床成矿系列与地球化学[M]. 西安: 地图出版社, 1996: 1–228.
Li Wenyuan. *Metalogenic Series and Geochemistry of Ni–Cu Sulfide Deposits in China*[M]. Xi'an: Xi'an Cartographic Publishing House, 1996: 1–228 (in Chinese).
- [12] Franklin J M, Gibson H L, Jonasson I R, et al. Volcanogenic massive sulfide deposits[J]. *Economic Geology* 100th anniversary volume, 2005, 98: 523–560.
- [13] 汤中立. 金川硫化铜镍矿床成矿模式[J]. 现代地质, 1990, 4(4): 55–64.
Tang Zhongli. Minerogenetic model of the Jinchuan copper and nickel sulfide deposit[J]. *Geoscience*, 1990, 4(4): 55–64 (in Chinese with English abstract).
- [14] Naldrett A J, Cabri L J. Ultramafic and related mafic rocks; their classification and genesis with special reference to the concentration of nickel sulfides and platinum-group elements[J]. *Economic Geology*, 1976, 71(7): 1131–1158.
- [15] Wu F Y, Wilde S A, Zhang G L, et al. Geochronology and petrogenesis of the post-orogenic Cu–Ni sulfide-bearing mafic–ultramafic complexes in Jilin Province, NE China[J]. *Journal of Asian Earth Sciences*, 2004, 23(5): 781–797.
- [16] 赵彦锋. 青海柴达木盆地西北缘牛鼻子梁镁铁质—超镁铁质层状岩体的地质特征与矿床成因[D]. 西安: 长安大学, 2013.
Zhao Yanfeng. Geological Character and Genesis of Niubiziliang Mafic–Ultramafic Layered Intrusion in the Northwest Margin of Qaidam Block, Qinghai, P.R. China[D]. Xi'an: Chang'an University, 2013 (in Chinese with English abstract).
- [17] Sláma J, Košler J, Condon D J, et al. Plešovice zircon—a new natural reference material for U–Pb and Hf isotopic microanalysis[J]. *Chemical Geology*, 2008, 249(1): 1–35.
- [18] Liu Y S, Hu Z C, Zong K Q, et al. Reappraisal and refinement of zircon U–Pb isotope and trace element analyses by LA–ICP–MS[J]. *Chinese Science Bulletin*, 2010, 55(15): 1535–1546.
- [19] 侯可军, 李延河, 田有荣. LA–MC–ICP–MS 锆石微区原位 U–Pb 定年技术[J]. 矿床地质, 2009, (4): 481–492.
Hou Kejun, Li Yanhe, Tian Yourong. In situ U–Pb zircon dating using laser ablation–multi ion counting–ICP–MS[J]. *Mineral Deposits*, 2009, (4): 481–492 (in Chinese with English abstract).
- [20] Belousova E, Griffin W L, O'reilly S Y, et al. Igneous zircon: trace element composition as an indicator of source rock type[J]. Contributions to mineralogy and petrology, 2002, 143(5): 602–622.
- [21] 汤中立. 中国镁铁、超镁铁岩浆矿床成矿系列的聚集与演化[J]. 地学前缘, 2004, 11(1): 113–119.
Tang Zhongli. The accumulation and evolution of metallogenetic series of the mafic–ultramafic magmatic deposits in China[J]. *Earth Science Frontiers*, 2004, 11(1): 113–119 (in Chinese with English abstract).
- [22] 汤中立, 钱壮志, 任秉琛, 等. 中国古生代成矿作用[M]. 北京: 地质出版社, 2005.
Tang Zhongli, Qian Zhuangzhi, Ren Bingchen, et al. *Paleozoic Mineralization in China*[M]. Beijing: Geological Publishing House, 2005 (in Chinese).
- [23] 张照伟, 李文渊, 高永宝, 等. 青海化隆基性–超基性岩带铜镍矿成矿条件与找矿潜力[J]. 西北地质, 2012, 45(1): 140–148.
Zhang Zhaowei, Li Wenyuan, Gao Yongbao, et al. Ni–Cu mineralization conditions of Hualong basic–ultrabasic rocks belt in Qinghai Province and its prospecting potentiality[J]. *Northwestern Geology*, 2012, 45(1): 140–148 (in Chinese with English abstract).
- [24] 张照伟, 李文渊, 高永宝, 等. 南祁连裕龙沟岩体 ID–TIMS 锆石 U–Pb 年龄及其地质意义[J]. 地质通报, 2012, 31(2): 455–462.
Zhang Zhaowei, Li Wenyuan, Gao Yongbao, et al. ID–TIMS zircon U–Pb age of Yulonggou intrusive rocks in southern Qilian Mountain and its geological significance[J]. *Geological Bulletin of China*, 2012, 31(2): 455–462 (in Chinese with English abstract).
- [25] Zhang Z W, Li W Y, Gao Y B, et al. Sulfide mineralization associated with arc magmatism in the Qilian Block, western China: zircon U–Pb age and Sr–Nd–Os–S isotope constraints from the Yulonggou and Yaqu gabbroic intrusions[J]. *Mineralium Deposita*, 2014, 49(2): 279–292.
- [26] Zhang M J, Kamo S L, Li C S, et al. Precise U–Pb zircon–baddeleyite age of the Jinchuan sulfide ore–bearing ultramafic intrusion, western China[J]. *Mineralium Deposita*, 2010, 45(1): 3–9.
- [27] Xu W C, Zhang H F, Liu X M. U–Pb zircon dating constraints on formation time of Qilian high-grade metamorphic rock and its tectonic implications[J]. *Chinese Science Bulletin*, 2007, 52(4): 531–538.
- [28] Zhou M F, Michael Lesher C, Yang Z X, et al. Geochemistry and petrogenesis of 270 Ma Ni–Cu–(PGE) sulfide–bearing mafic intrusions in the Huangshan district, Eastern Xinjiang, Northwest China: implications for the tectonic evolution of the Central Asian orogenic belt[J]. *Chemical Geology*, 2004, 209(3): 233–257.
- [29] Qin K Z, Su B X, Sakyi P A, et al. SIMS zircon U–Pb geochronology and Sr–Nd isotopes of Ni–Cu–Bearing Mafic–Ultramafic Intrusions in Eastern Tianshan and Beishan in correlation with flood basalts in Tarim Basin (NW China): Constraints on a ca. 280 Ma mantle plume[J]. *American Journal of Science*, 2011, 311(3): 237–260.
- [30] Han B F, Ji J Q, Song B, et al. SHRIMP zircon U–Pb ages of

- Kalatongke No. 1 and Huangshandong Cu–Ni–bearing mafic–ultramafic complexes, North Xinjiang, and geological implications[J]. Chinese Science Bulletin, 2004, 49(22): 2424–2429.
- [31] 韩宝福, 季建清, 宋彪, 等. 新疆喀拉通克和黄山东含铜镍矿镁铁–超镁铁杂岩体的 SHRIMP 锆石 U–Pb 年龄及其地质意义[J]. 科学通报, 2005, 49(22): 2324–2328.
Han Baofu, Ji Jianqing, Song Biao, et al. Zircon U–Pb SHRIMP ages of the mafic–ultramafic complexes from the Kalatongke and Huangshandong Cu–Ni sulfide deposits, Xingjiang Province, and their tectonic significance[J]. Chinese Science Bulletin, 2005, 49 (22): 2324–2328 (in Chinese).
- [32] 马启贵, 肖文交, 韩春明, 等. 新疆东天山白石泉铜镍矿床基性–超基性岩体锆石 U–Pb 同位素年龄、地球化学特征及其对古亚洲洋闭合时限的制约[J]. 岩石学报, 2006, 22(1): 153–162.
Mao Qigui, Xiao Wenjiao, Han Chunming, et al. Zircon U–Pb age and the geochemistry of the Baishiquan mafic–ultramafic complex in the Eastern Tianshan, Xinjiang Province: constraints on the closure of the Paleo– Asian Ocean[J]. Acta Petrologica Sinica, 2006, 22(1): 153–162 (in Chinese with English abstract).
- [33] 孙涛, 钱壮志, 汤中立, 等. 新疆葫芦铜镍矿床锆石 U–Pb 年代学、铂族元素地球化学特征及其地质意义[J]. 岩石学报, 2010, 26(11): 3339–3349.
Sun Tao, Qian Zhuangzhi, Tang Zhongli, et al. Zircon U–Pb chronology, platinum group element geochemistry characteristics of Hulu Cu– Ni deposit, East Xinjiang, and its geological significance[J]. Acta Petrologica Sinica, 2010, 26(11): 3339–3349 (in Chinese with English abstract).
- [34] 王登红, 李建康, 王成辉, 等. 与峨眉地幔柱有关年代学研究的新进展及其意义[J]. 矿床地质, 2007, 26(5): 550–556.
Wang Denghong, Li Jiankang, Wang Chenghui, et al. New advances in geochronologic study related to Emei mantle plume and their significance[J]. Mineral deposits, 2007, 26(5): 550–556 (in Chinese with English abstract).
- [35] Wang C Y, Zhou M F, Keays R R. Geochemical constraints on the origin of the Permian Baimazhai mafic–ultramafic intrusion, SW China[J]. Contributions to mineralogy and petrology, 2006, 152 (3): 309–321.
- [36] Sun X M, Wang S W, Sun W D, et al. PGE geochemistry and Re–Os dating of massive sulfide ores from the Baimazhai Cu–Ni deposit, Yunnan province, China[J]. Lithos, 2008, 105(1): 12–24.
- [37] Zhong H, Zhu W G, Chu Z Y, et al. SHRIMP U–Pb zircon geochronology, geochemistry, and Nd– Sr isotopic study of contrasting granites in the Emeishan large igneous province, SW China[J]. Chemical Geology, 2007, 236(1): 112–133.
- [38] Li C S, Zhang Z W, Li W Y, et al. Geochronology, petrology and Hf–S isotope geochemistry of the newly–discovered Xiarihamu magmatic Ni–Cu sulfide deposit in the Qinghai–Tibet plateau, western China[J]. Lithos, 2015, 216(2): 224–240.
- [39] 张照伟, 李文渊, 高永宝, 等. 南祁连亚曲含镍铜矿基性杂岩体形成年龄及机制探讨[J]. 地球学报, 2012, 33(6): 925–935.
Zhang Zhaowei, Li Wenyuan, Gao Yongbao, et al. The Formation Age of the Yaqu Ni– Cu Bearing Basic Complex in Southern Qilian Mountain and a Discussion on Its Mechanism[J]. Acta Geoscientica Sinica, 2012, 33(6): 925– 935 (in Chinese with English abstract).
- [40] 杨经绥. 柴达木盆地北缘早古生代高压–超高压变质带中发现典型超高压矿物—柯石英[J]. 地质学报, 2001, 75(2): 175–179.
Yang Jingsui. Discovery of Coesite in the North Qaidam Early Paleozoic Ultrahigh– high Pressure (UHP– HP) Metamorphic Belt, NW China[J]. Acta Geologica Sinica, 2001, 75(2): 175–179 (in Chinese with English abstract).
- [41] Song S G, Yang J S, Xu Z Q, et al. Metamorphic evolution of the coesite–bearing ultrahigh–pressure terrane in the North Qaidam, Northern Tibet, NW China[J]. Journal of metamorphic Geology, 2003, 21(6): 631–644.
- [42] 袁桂邦, 张宝华. 柴北缘绿梁山地区辉长岩的锆石 U–Pb 年龄及意义[J]. 前寒武纪研究进展, 2002, 25(1): 36–40.
Yuan Guibang, Zhang Baohua. Zircon U–Pb age of the Gabbros in Luliangshan Area on the Northern Margin of Qaidam Basin and its Geological Implication[J]. Progress in Precambrian Research, 2002, 25(1): 36–40 (in Chinese with English abstract).
- [43] 陈丹玲, 孙勇, 刘良, 等. 柴北缘鱼卡河榴辉岩的超高压变质年龄: 锆石 LA–ICP–MS 微区定年[J]. 中国科学(D辑), 2007, 37 (A01): 279–287.
Chen Danling, Sun Yong, Liu Liang, et al. In situ LA–ICP–MS zircon U–Pb age of ultrahigh–pressure eclogites in the Yukahe area, Northern margin of the Qaidam Basin. [J]. Science in China (Series D), 2007, 37(A01): 279–287 (in Chinese).
- [44] 陈丹玲, 孙勇, 刘良. 柴北缘野马滩超高压榴辉岩中副片麻岩夹层的锆石 U–Pb 定年及其地质意义[J]. 岩石学报, 2008, 24(5): 1059–1067.
Chen Danling, Sun Yong, Liu Liang. Zircon U– Pb dating of paragneiss interbed in the UHP edogite from Yematan area, the North Qaidam UHP terrane, NW China[J]. Acta Petrologica Sinica, 2008, 24(5): 1059– 1067 (in Chinese with English abstract).
- [45] 张建新, 杨经绥. 柴北缘榴辉岩的峰期和退变质年龄: 来自 U–Pb 及 Ar–Ar 同位素测定的证据[J]. 地球化学, 2000, 29(3): 217–222.
Zhang Jianxin, Yang Jingsui. Peak and retrograde age of eclogites at the northern margin of Qaidam basin, northwestern China: Evidences from U–Pb and Ar–Ar dates[J]. Geochimica, 2000, 29 (3): 217–222 (in Chinese with English abstract).
- [46] 郝国杰, 郑建康. 柴北缘沙柳河榴辉岩岩石学及年代学初步研究[J]. 前寒武纪研究进展, 2001, 24(3): 154–162.
Hao Guojie, Zheng Jiankang. Determination and Significance of Eclogite on Shaliuhe, in the North Margin of the Qaidam

- Basin[J]. *Progress in Precambrian Research*, 2001, 24(3): 154–162 (in Chinese with English abstract).
- [47] 刘良, 车自成, 罗金海, 等. 阿尔金山西段榴辉岩的确定及其地质意义[J]. *科学通报*, 1996, 41(16): 1485–1488.
Liu Liang, Che Zicheng, Luo Jinhai, et al. Recognition and implication of eclogite in the western Altun Mountains, Xinjiang. [J]. *Chines Science Bulletin*, 1996, 41(16): 1485–1488 (in Chinese).
- [48] 校培喜, 王永和, 张汉文, 等. 阿尔金山中段高压-超高压带(含菱镁矿)石榴子石二辉橄榄岩的发现及其地质意义[J]. *西北地质*, 2001, 34(4): 67–74.
Xiao Peixi, Wang Yonghe, Zhang Hanwen, et al. The discovery of magnesite-bearing garnet lherzolite of high-ultrahigh pressure belt and its geological significance in the middle section of Altyn Tagh[J]. *Northwestern Geology*, 2001, 34(4): 67–74 (in Chinese with English abstract).
- [49] 覃小峰, 夏斌, 李江, 等. 阿尔金南缘构造带西段早古生代绿片岩的地球化学特征及构造环境[J]. *中国地质*, 2007, 34(5): 799–807.
Qin Xiaofeng, Xia Bin, Li Jiang, et al. Geochemical characteristics and tectonic setting of the Early Paleozoic greenschist in the western segment of the southern Altyn Tagh marginal tectonic belt[J]. *Geology in China*, 2007, 34(5): 799–807 (in Chinese with English abstract).
- [50] 许志琴, 杨经绥, 张建新, 等. 阿尔金断裂两侧构造单元的对比及岩石圈剪切机制[J]. *地质学报*, 1999, 73(3): 193–205.
Xu Zhiqin, Yang Jingsui, Zhang Jianxin, et al. Comparison of the tectonic units on both sides of the Altyn Tagh fault and the mechanism of lithospheric shearing[J]. *Acta Geologica Sinica*, 1999, 73(3): 193–205 (in Chinese).
- [51] 葛肖虹, 刘俊来. 北祁连造山带的形成与背景[J]. *地学前缘*, 1999, 6(4): 223–230.
Ge Xiaohong, Liu Junlai. Formation and tectonic background of the northern Qilian orogenic belt[J]. *Earth Science Frontiers*, 1999, 6(4): 223–230 (in Chinese with English abstract).
- [52] 杨经绥, 许志琴, 张建新, 等. 中国主要高压-超高压变质带的地构造背景及俯冲/折返机制的探讨[J]. *岩石学报*, 2009, (7): 1529–1560.
Yang Jingsui, Xu Zhiqin, Zhang Jianxin, et al. Tectonic setting of main high- and ultrahigh-pressure metamorphic belts in China and adjacent region and discussion on their subduction and exhumation mechanism[J]. *Acta Petrologica Sinica*, 2009, (7): 1529–1560 (in Chinese with English abstract).
- [53] 许志琴, 杨经绥, 鲍少丞, 等. 中国大陆构造及动力学若干问题的认识[J]. *地质学报*, 2010, 84(1): 1–29.
Xu Zhiqin, Yang Jingsui, Ji Shaocheng, et al. On the Continental Tectonics and Dynamics of China[J]. *Acta Geologica Sinica*, 2010, 84(1): 1–29 (in Chinese with English abstract).
- [54] 赖绍聪, 邓晋福, 赵海玲. 柴达木北缘古生代蛇绿岩及其构造意义[J]. *现代地质*, 1996, 10(1): 18–28.
Lai Shaocong, Deng Jinfu, Zhao Hailing. Paleozoic ophiolites and its tectonic significance on north margin of Qaidam Basin[J]. *Geoscience*, 1996, 10(1): 18–28 (in Chinese with English abstract).
- [55] 史仁灯, 杨经绥, 吴才来, 等. 柴达木北缘超高压变质带中的岛弧火山岩[J]. *地质学报*, 2004, 78(1): 52–64.
Shi Rendeng, Yang Jingsui, Wu Cailai, et al. Island Arc Volcanic Rocks in the North Qaidam UHP Metamorphic Belt[J]. *Acta Geologica Sinica*, 2004, 78(1): 52–64 (in Chinese with English abstract).
- [56] 吴才来, 邵源红, 吴锁平, 等. 柴北缘西段花岗岩锆石 SHRIMP U-Pb 定年及其岩石地球化学特征[J]. *中国科学(D辑)*, 2008, 38(8): 930–949.
Wu Cailai, Hao Yuanhong, Wu Suoping, et al. Geochemistry and zircon SHRIMP U-Pb dating of granitoids from the west segment of the North Qaidam[J]. *Science in China (Series D)*, 2008, 52(11): 1771–1790.
- [57] 宋述光, 牛耀龄, 张立飞, 等. 大陆造山运动: 从大洋俯冲到大陆俯冲、碰撞、折返的时限—以北祁连山, 柴北缘为例[J]. *岩石学报*, 2009, 25(9): 2067–2077.
Song Shuguang, Niu Yaoling, Zhang Lifei, et al. Time constraints on orogenesis from oceanic subtraction to continental subduction, collision, and exhumation: An example from North Qilian and North Qaidam HP-UHP belts[J]. *Acta Petrologica Sinica*, 2009, 25(9): 2067–2077 (in Chinese with English abstract).
- [58] 周宾, 郑有业, 许荣科, 等. 青海柴达木山岩体 LA-ICP-MS 锆石 U-Pb 定年及 Hf 同位素特征[J]. *地质通报*, 2013, 32(7): 1027–1034.
Zhou Bin, Zhen Youye, Xu Rongke, et al. LA-ICP-MS zircon U-Pb dating and Hf isotope geochemical characteristics of Qaidamshan intrusive body[J]. *Geological Bulletin of China*, 2013, 32(7): 1027–1034.